

---

# Model-Free Assessment of Simulator Fidelity via Quantile Curves

---

**Garud Iyengar**   **Yu-Shiou Willy Lin**   **Kaizheng Wang**  
Department of Industrial Engineering and Operations Research  
Columbia University  
New York, NY 10027

garud@ieor.columbia.edu   yl5782@columbia.edu   kaizheng.wang@columbia.edu.

## Abstract

1        Simulation is now pervasive, arising from manufacturing to LLM-driven appli-  
2        cations in research, education, and consumer surveys. Yet, fully characterizing  
3        the discrepancy between simulators and ground truth remains challenging. We  
4        propose a computationally tractable method to estimate the quantile function of the  
5        discrepancy between the simulated and ground-truth distributions. The approach  
6        does not impose any modeling assumptions on the simulator and it applies broadly  
7        across many parameter families: from Bernoulli and multinomial to continuous,  
8        vector-valued settings. The resulting quantile curve supports risk-aware summaries  
9        (e.g., VaR/CVaR) and comparison of simulators or prompts performance. We  
10       illustrate our framework through an application assessing LLM simulation fidelity  
11       on the OpinionQA dataset, augmented with simulations spanning seven LLMs.

## 12    1 Introduction

13       The adoption of simulators across operations and manufacturing, agent-based modeling in social-  
14       science research, user surveys, and education/training [20, 10, 2, 1] has accelerated with recent  
15       advances in artificial intelligence (AI). At the platform level, industry ecosystems such as NVIDIA  
16       Omniverse and Earth-2 exemplify the push toward high-fidelity, AI-enabled digital twins. Collectively,  
17       these developments fuel the sustained growth in modeling and simulation across domains.

18       Against this backdrop, it becomes increasingly important to understand the discrepancy between  
19       simulation outputs and the real-world. Such discrepancies are documented across many domains:  
20       the behavior of large language models (LLMs) , model discrepancy in computing systems, and  
21       sim-to-real gap in robotics [5, 4, 14, 17, 13]. To quantify this gap, a large body of work performs  
22       Bayesian inference on simulator discrepancy [9]. Their validity hinges on modeling assumptions.  
23       On the other hand, recent studies of LLMs yield a variety of model-agnostic discrepancy measures.  
24       They are numerical summaries of the overall error [15] or the severity at a given quantile level [8]. To  
25       provide flexible and comprehensive analytics, we propose a model-free procedure to approximate the  
26       entire quantile function of the discrepancy between the real-world and simulated distributions. Our  
27       work shares a similar spirit with conformal inference approaches [18, 3]. However, they typically  
28       target pointwise coverage rather than a full distributional characterization, which is a gap we aim to  
29       fill.

30       Ideally, one wants to recover the quantile function for a specified discrepancy measure between the  
31       real-world and the simulated distributions. The quantile function directly leads to confidence intervals  
32       for the estimators, and risk summaries, e.g. VaR/CVaR. In practice, we only observe finite samples of  
33       the real-world and simulated outcomes, and therefore, the true quantile function is not computable.  
34       We construct a model-free conservative estimate for the quantile function, and prove that our estimate  
35       comes with finite-sample guarantees for any desired  $\alpha$ -quantile.

36 Our contributions are twofold:

- 37 1. Our procedure is model-free in that it does not impose any parametric assumptions on either  
38 the simulator or the ground truth; therefore, it can be applied to black-box simulators.
- 39 2. Since our procedure results in a quantile *function*, we can produce a range of different  
40 summaries – from means to tail-risk measures.

41 The remainder of the paper proceeds as follows. In Section 2 we present a motivating example, and  
42 formally state the problem. In Section 3 we present the main theoretical result, and in Section 4 we  
43 discuss an application of our methodology. In Section 5 we conclude by discussing future directions.

## 44 2 Problem Formulation and Motivating Example

45 In this section, we start with a concrete use case that motivates our formulation, and then formally  
46 define the quantile estimation problem. Although the terminology below is specific to the example  
47 use case, the setting can be generalized. See Appendix B for more examples.

48 Suppose a media research company plans to survey customers on a particular topic with multinomial  
49 outcomes (eg. “Agree”, “Neutral”, “Disagree”). The company wants to estimate the customer opinion  
50 before committing resources for an expensive population study. The company has access to a database  
51 of past questions and human answers, and have been training an LLM-based “digital twin” for its  
52 customer base. By querying this digital twin with the new question, the company can generate an  
53 estimate for the mean response for the new question. The problem now facing the company is to  
54 characterize how close this estimate is to the true population mean. Can one provide a confidence  
55 interval for the true value? Or, better yet, estimate the quantile function for a suitable discrepancy  
56 measure between the simulator and population estimates? This work addresses precisely this problem.

57 To formally describe the discrepancy between simulator (LLM) and ground truth (human population),  
58 and the theoretical challenges we are facing, we consider two levels of randomness in this problem.

59 First, scenarios (questions) are drawn as  $\psi \sim \Psi$ . A real system (human) is characterized by  $z \in \mathcal{Z}$   
60 with a population distribution  $\mathcal{P}$  over the latent profile state  $\mathcal{Z}$ . For each pair  $(\psi, z)$ , the real system  
61 (human population) produces an categorical outcome  $Y^{\text{gt}}$ , with conditional distribution  $Q^{\text{gt}}(\cdot | z, \psi)$   
62 over a space  $\mathcal{Y} := \{y \in \mathbb{N}^d : \sum_{i=1}^d y_i = 1\}$ . The simulator (LLM) produces an outcome  
63  $Y^{\text{sim}}$  with conditional distribution  $Q^{\text{sim}}(z^{\text{sim}}, \psi, r)$  over the same outcome space  $\mathcal{Y}$ , where the  
64  $z^{\text{sim}} \in \mathcal{P}^{\text{sim}}$  denotes the i.i.d. synthetic profile that is fed into the LLM, and  $r$  denotes LLM settings,  
65 including prompting strategy, hyperparameters, and other API settings<sup>1</sup> In our example,  $Q^{\text{gt}}(\cdot | z, \psi) =$   
66  $\text{Categorical}(\Pi^{\text{gt}}(z, \psi))$ , where  $\Pi^{\text{gt}}(\psi, z) := (Q^{\text{gt}}(\{1\} | z, \psi), \dots, Q^{\text{gt}}(\{d\} | z, \psi)) \in \mathcal{P}^d$  and  
67  $\mathcal{P}^d := \{u \in [0, 1]^d : \sum_{i=1}^d u_i = 1\}$ . For any question  $\psi$ , we can marginalize the population effect,  
68 hence denote by  $Q^{\text{gt}}(\cdot | \psi) = \mathbb{E}_{z \sim \mathcal{P}}[Q^{\text{gt}}(\cdot | z, \psi)]$ , the conditional distribution of outcome  $Y^{\text{gt}}$  given  
69  $\psi$ . Let  $p(\psi)$  be a population statistic of interest, which is a functional of the conditional distribution  
70  $Q^{\text{gt}}(\cdot | \psi)$  and lives in a parameter space  $\Theta$ , in this case  $= \mathcal{P}^d$ , and simulator can be defined similarly  
71 under the simulator population  $\mathcal{P}^{\text{sim}}$ , summing up:

$$p(\psi) := \mathbb{E}_{y \sim Q^{\text{gt}}}[y] = \mathbb{E}_{z \sim \mathcal{P}}[\Pi^{\text{gt}}(\psi, z)] \in \Theta, \quad q(\psi) := \mathbb{E}_{z \sim \mathcal{P}^{\text{sim}}}[\Pi^{\text{sim}}(\psi, z)] \in \Theta.$$

72 Second, we only observe finite samples per question. For each  $j \in [m]$ , we are given a question  
73  $\psi_j \sim \Psi$  and  $n_j$  i.i.d. profiles  $z_{j,1:n_j} \sim \mathcal{P}$ , with which we observe  $n_j$  ground-truth outcomes  
74  $y_{j,i}^{\text{gt}} \sim Q^{\text{gt}}(\cdot | z_{j,i}, \psi_j)$ . Next, we generate  $k$  simulator outcomes  $y_{j,\ell}^{\text{sim}} \sim Q^{\text{sim}}(\cdot | z^{\text{sim}}, \psi_j, r)$  using a  
75 simulation pool  $z_{j,1:k}^{\text{sim}} \sim \mathcal{P}^{\text{sim}}$  with fixed  $k$  across  $j$  to standardize simulator sampling. In addition, let  
76  $\hat{p}_j$  and  $\hat{q}_j$  be estimators of  $p(\psi_j)$  and  $q(\psi_j)$ . Concluding, the dataset is  $\mathcal{D} = \{(\psi_j, \hat{p}_j, \hat{q}_j, n_j, k)\}_{j=1}^m$ .  
77 Notice that we set  $k$  to be fixed across  $j$  so that  $\{\hat{q}_j\}_{j=1}^m$  are identically distributed, which can be  
78 justified since sample collection for simulators are relatively inexpensive.

79 On a  $\psi \sim \Psi$ , the discrepancy between simulated and real output distributions is defined as  
80  $L(p(\psi), q(\psi))$ , where  $L : \Theta \times \Theta \rightarrow [0, \infty]$  is a discrepancy function. Our method is agnostic

<sup>1</sup>We keep  $r$  fixed during calibration so that variation in  $\hat{q}_j$  reflects scenario differences rather than encoding drift or model choice; choosing a different  $r$  effectively defines a different simulator.

81 to the choice of  $L$  and allows practitioners to choose one that suits their use, such as the Kullback-  
 82 Leibler (KL) divergence for categorical outputs. With the above setup, we can now formally state our  
 83 goal:

84 Construct a function  $V(\cdot, \mathcal{D}) : [0, 1] \rightarrow \mathbb{R}$  from the data  $\mathcal{D}$  such that the coverage guarantee for a  
 85 new  $\psi$

$$\mathbb{P}_{\psi \sim \Psi}(L(p(\psi), \hat{q}(\psi)) \leq V(\alpha, \mathcal{D}) | \mathcal{D}) \geq 1 - \alpha - \varepsilon_m, \quad \forall \alpha \in [0, 1],$$

86 holds with high probability over the draw of  $\mathcal{D}$ . The quantity  $\varepsilon_m$  should vanish as  $m$  tends to infinity.

### 87 3 Main Result

88 We introduce our method for constructing such  $V$  and then provide theoretical guarantees. Recall  
 89 that our data  $\mathcal{D}$  consists of  $m$  questions; the  $j$ -th question has population parameters  $p(\psi_j)$  and  $q(\psi_j)$   
 90 in the real and simulated systems;  $\hat{p}_j$  and  $\hat{q}_j$  are their point estimates. Our procedure has two steps:

- 91 1. For each  $j$ , compute a confidence set  $\mathcal{C}_j(\hat{p}_j)$  on  $p_j$ , and calculate the pseudo-discrepancy  
 92  $\hat{\Delta}_j := \sup_{u \in \mathcal{C}_j(\hat{p}_j)} L(u, \hat{q}_j)$ .
- 93 2. Denote  $\hat{V}_m(\alpha) :=$  the empirical  $\alpha$ -quantile of  $\{\hat{\Delta}_j\}_{j=1}^m$ .

94 The key design choice in our methodology is the construction of  $\mathcal{C}_j(\cdot)$ . Consistent with our motivating  
 95 example, we illustrate with a multinomial setting.

96 **Example 1 (Multinomial Confidence Set)** Under our problem formulation, we have multinomial  
 97 outcomes with  $\Theta = \mathcal{P}^d := \{u \in [0, 1]^d : \sum_{i=1}^d u_i = 1\}$  and denote KL divergence as  $\text{KL}(\cdot \| \cdot)$ . For  
 98 any  $\gamma \in (0, 1)$ , the set

$$\mathcal{C}_j(\hat{p}_j) := \left\{ u \in \mathcal{P}^d : \text{KL}(\hat{p}_j \| u) \leq \frac{d-1}{n_j} \log(2(d-1)/\gamma) \right\}$$

99 covers  $p_j$  with probability at least  $\gamma$ .

100 The validity of this confidence set is proved in Lemma A.5. In addition to multinomial outcomes,  
 101 Appendix A provides the bound required for Bernoulli models and more generally, exponential family,  
 102 covering additional classes of simulation outputs. With the above methodology, we can now state the  
 103 main theoretical guarantee. We introduce two assumptions on which it relies.

104 **Assumption 1 (Independent data)** Scenarios  $\psi_j \in \Psi$  are drawn i.i.d. from  $\Psi$ . In addition, given  
 105  $(\psi_1, \dots, \psi_m)$ , the pairs  $\mathcal{D} = \{(\mathcal{D}_j^{\text{gt}}, \mathcal{D}_j^{\text{sim}})\}_{j=1}^m$  are independent with  $\mathcal{D}_j^{\text{gt}} \perp\!\!\!\perp \mathcal{D}_j^{\text{sim}}$  conditional on  
 106  $\psi_j$ , and a new  $(\psi, \mathcal{D}^{\text{sim}})$  is independent of  $\mathcal{D}$ .

107 **Assumption 2 (Regular Discrepancy)** The discrepancy  $L : \Theta \times \Theta \rightarrow [0, \infty)$  is jointly continuous  
 108 on  $\Theta \times \Theta$  and satisfies  $L(u, u) = 0$  for all  $u \in \Theta$ .

109 We are now equipped to introduce the main theorem. A complete proof is in Appendix C.

110 **Theorem 3.1** Under assumption 1 and 2, define the per-scenario discrepancy (unobservable)  $\Delta(\psi)$   
 111 and the pseudo-discrepancy (observable)  $\hat{\Delta}(\psi)$  by

$$\Delta(\psi) := L(p(\psi), \hat{q}(\psi)), \quad \hat{\Delta}_j := \sup_{u \in \mathcal{C}_j(\hat{p}_j)} L(u, \hat{q}_j),$$

112 where  $\mathcal{C}_j(\hat{p}_j) \subset \Theta$  are data-driven compact confidence sets satisfying  $\mathbb{P}(p_j \in \mathcal{C}_j(\hat{p}_j) | \psi_j, n_j) \geq \frac{1}{2}$ .  
 113 Then, for any  $\alpha \in (0, 1)$ , with probability at least  $1 - \delta$  over  $\mathcal{D}$ , we have the following guarantee:

$$\mathbb{P}_{\psi \sim \Psi}(\Delta(\psi) \leq \hat{V}_m(1 - \frac{\alpha}{2}) | \mathcal{D}) \geq 1 - \alpha - \frac{C(\alpha, m, \delta)}{\sqrt{m}},$$

114 where  $C(\alpha, m, \delta) = \sqrt{2\alpha \log \frac{2m}{\delta} + \frac{(\log \frac{2m}{\delta})^2 + 4 \log \frac{2m}{\delta}}{m}} + \frac{\log \frac{2m}{\delta} + 2}{\sqrt{m}} + \sqrt{\frac{\log(4/\delta)}{2}}$ , hence the remainder  
 115 is  $O(\sqrt{(\log m)/m})$  as  $m \rightarrow \infty$  for fixed  $\alpha$ .

116 **4 Application: LLM Fidelity Profiling**

117 We apply the methodology from Section 3 to real data. Our primary dataset is OpinionQA [16],  
 118 built from the Pew Research’s American Trends Panel, which consists of the US population’s  
 119 responses to survey questions spanning topics such as racial equity, security, and technology. We  
 120 adopt the preprocessed version curated by [8], which includes 385 distinct questions and 1,476,868  
 121 responses from at least 32,864 people. Each question has 5 choices, corresponding to the order  
 122 sentiments, which is a multinomial setting. We can construct confidence sets  $\mathcal{C}_j$  for multinomial  
 123 vectors by adopting Example 1 with  $d = 5$ . OpinionQA also provides individual-level covariates  
 124 such as gender, age, socioeconomic status, religious affiliation, and marital status, and more, which  
 125 are used to construct synthetic profiles. Under the same problem formulation, the authors of [8]  
 126 compute  $\{\hat{p}_j, \hat{q}_j\}_{j=1}^{385}$  for seven LLMs: GPT-3.5-TURBO (gpt-3.5-turbo), GPT-4O (gpt-4o), and  
 127 GPT-4O-MINI (gpt-4o-mini); CLAUDE 3.5 HAIKU (claude-3-5-haiku-20241022); LLAMA  
 128 3.3 70B (Llama-3.3-70B-Instruct-Turbo); MISTRAL 7B (Mistral-7B-Instruct-v0.3);  
 129 DEEPSEEK-V3 (DeepSeek-V3), and constructed a baseline random simulator that selects uniformly  
 130 among the available answer choices. A more detailed exploration into the OpinionQA dataset and  
 131 the simulation procedure can be found in [8]. We also provide the same procedure onto a Bernoulli  
 132 setting using the EEDI dataset, details can be found in Appendix D.

133 We apply our methodology to produce a fidelity profile for each candidate LLM  $\ell$ . We use total  
 134 variation as the discrepancy measure,  $L(p, q) = \frac{1}{2} \|p - q\|_1$ , and set  $\delta = 0.05$ . In addition, we set the  
 135 simulation budget  $k = 100$ , the result is presented in Figure 1.

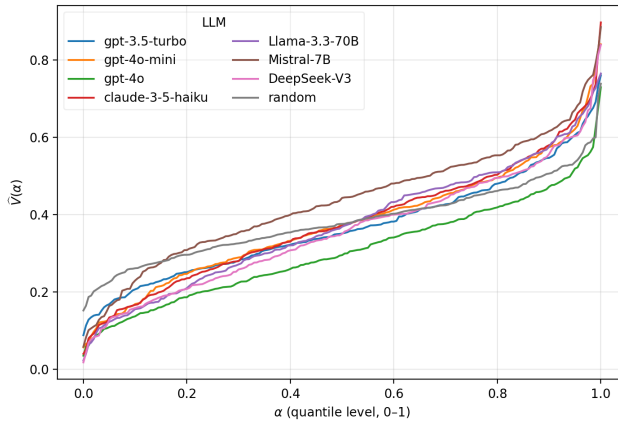


Figure 1: Quantile fidelity profiles  $\hat{V}(\alpha)$  across LLMs.

136 Figure 1 compares models by how tightly their synthetic outcomes track the human distribution across  
 137 items. We plot  $\hat{V}_\ell(\alpha)$  against  $\alpha$ , where lower-flatter curves indicate uniformly small discrepancies,  
 138 while elbows reveal rare but severe misses. GPT-4O lies lowest across most quantiles, indicating the  
 139 most reliable alignment, with MISTRAL 7B clearly performing worse. Notably, the simulator curves  
 140 are steeper than the random benchmark, indicating question-dependent alignment and less uniform  
 141 discrepancies. This suggests the simulators may require further fine-tuning to achieve more uniform  
 142 discrepancy levels across this set of questions.

143 **5 Discussion**

144 We present a model-free estimator of the quantile function that makes no parametric assumptions on  
 145 either the simulator or the ground truth, delivers finite-sample guarantees for any desired  $\alpha$ -quantile,  
 146 and supports flexible summaries from means to tail-risk measures. Several promising directions  
 147 remain: first, our proof relies on DKW-type concentration—often conservative for small  $m$ —and  
 148 a grid-uniform step that further loosens constants; tightening these bounds is an immediate target.  
 149 Second, many applications involve temporally dependent, dynamic simulation processes; extending  
 150 our static framework to dynamic settings would broaden applicability. Third, our analysis assumes  
 151 i.i.d. scenarios, whereas covariate shift or endogenous sampling may invalidate marginal guarantees;  
 152 addressing such distribution shifts is an important avenue for future work.

## References

- 153
- 154 [1] G. Aher, R. I. Arriaga, and A. T. Kalai. Using large language models to simulate multiple humans  
155 and replicate human subject studies. In *Proceedings of the 40th International Conference on*  
156 *Machine Learning*, ICML'23. JMLR.org, 2023.
- 157 [2] L. P. Argyle, E. C. Busby, N. Fulda, J. R. Gubler, C. Rytting, and D. Wingate. Out of one, many:  
158 Using language models to simulate human samples. *Political Analysis*, 31(3):337–351, 2023.
- 159 [3] S. Bates, A. Angelopoulos, L. Lei, J. Malik, and M. Jordan. Distribution-free, risk-controlling  
160 prediction sets. *Journal of the ACM (JACM)*, 68(6):1–34, 2021.
- 161 [4] E. Durmus, K. Nguyen, T. I. Liao, N. Schiefer, A. Askill, A. Bakhtin, C. Chen, Z. Hatfield-  
162 Dodds, D. Hernandez, N. Joseph, et al. Towards measuring the representation of subjective  
163 global opinions in language models. *arXiv preprint arXiv:2306.16388*, 2023.
- 164 [5] Y. Gao, D. Lee, G. Burtch, and S. Fazelpour. Take caution in using llms as human surrogates.  
165 *Proceedings of the National Academy of Sciences*, 122(24):e2501660122, 2025.
- 166 [6] J. He-Yueya, W. A. Ma, K. Gandhi, B. W. Domingue, E. Brunskill, and N. D. Goodman.  
167 Psychometric alignment: Capturing human knowledge distributions via language models. *arXiv*  
168 *preprint arXiv:2407.15645*, 2024.
- 169 [7] W. Hoeffding. Probability inequalities for sums of bounded random variables. *Journal of the*  
170 *American Statistical Association*, 58(301):13–30, 1963.
- 171 [8] C. Huang, Y. Wu, and K. Wang. Uncertainty quantification for LLM-based survey simulations.  
172 In *Forty-second International Conference on Machine Learning*, 2025.
- 173 [9] M. C. Kennedy and A. O'Hagan. Bayesian calibration of computer models. *Journal of the*  
174 *Royal Statistical Society: Series B (Statistical Methodology)*, 63(3):425–464, 2001.
- 175 [10] C. Macal. Everything you need to know about agent-based modelling and simulation. *Journal*  
176 *of Simulation*, 10:144–156, 05 2016.
- 177 [11] J. Mardia, J. Jiao, E. Tanczos, R. D. Nowak, and T. Weissman. Concentration inequalities for  
178 the empirical distribution of discrete distributions: beyond the method of types. *Information*  
179 *and Inference: A Journal of the IMA*, 9(4):813–850, 11 2019.
- 180 [12] P. Massart. The tight constant in the dvoretzky-kiefer-wolfowitz inequality. *The annals of*  
181 *Probability*, pages 1269–1283, 1990.
- 182 [13] X. B. Peng, M. Andrychowicz, W. Zaremba, and P. Abbeel. Sim-to-real transfer of robotic  
183 control with dynamics randomization. In *2018 IEEE international conference on robotics and*  
184 *automation (ICRA)*, pages 3803–3810. IEEE, 2018.
- 185 [14] C. J. Roy and W. L. Oberkampf. A comprehensive framework for verification, validation, and  
186 uncertainty quantification in scientific computing. *Computer Methods in Applied Mechanics*  
187 *and Engineering*, 200(25):2131–2144, 2011.
- 188 [15] S. Santurkar, E. Durmus, F. Ladhak, C. Lee, P. Liang, and T. Hashimoto. Whose opinions do  
189 language models reflect? In *Proceedings of the 40th International Conference on Machine*  
190 *Learning*, ICML'23. JMLR.org, 2023.
- 191 [16] S. Santurkar, E. Durmus, F. Ladhak, C. Lee, P. Liang, and T. Hashimoto. Whose opinions do  
192 language models reflect? In *Proceedings of the 40th International Conference on Machine*  
193 *Learning*, ICML'23. JMLR.org, 2023.
- 194 [17] J. Tobin, R. Fong, A. Ray, J. Schneider, W. Zaremba, and P. Abbeel. Domain randomization  
195 for transferring deep neural networks from simulation to the real world. In *2017 IEEE/RSJ*  
196 *international conference on intelligent robots and systems (IROS)*, pages 23–30. IEEE, 2017.
- 197 [18] V. Vovk, A. Gammerman, and G. Shafer. *Algorithmic Learning in a Random World*. Springer-  
198 Verlag, Berlin, Heidelberg, 2005.

- 199 [19] Z. Wang, A. Lamb, E. Saveliev, P. Cameron, J. Zaykov, J. M. Hernandez-Lobato, R. E. Turner,  
 200 R. G. Baraniuk, E. Craig Barton, S. Peyton Jones, S. Woodhead, and C. Zhang. Results and  
 201 insights from diagnostic questions: The neurips 2020 education challenge. In H. J. Escalante  
 202 and K. Hofmann, editors, *Proceedings of the NeurIPS 2020 Competition and Demonstration*  
 203 *Track*, volume 133 of *Proceedings of Machine Learning Research*, pages 191–205. PMLR,  
 204 06–12 Dec 2021.
- 205 [20] L. Zhang, L. Zhou, L. Ren, and Y. Laili. Modeling and simulation in intelligent manufacturing.  
 206 *Computers in Industry*, 112:103123, 2019.

## 207 A Useful Lemmas

208 **Lemma A.1** (*Dvoretzky–Kiefer–Wolfowitz (DKW) Inequality via [12]*)

209 Let  $X_1, X_2, \dots, X_n$  be i.i.d. real-valued random variables with cumulative distribution function  
 210 (CDF)  $F^*$ , and let  $\hat{F}_n$  be the empirical distribution function defined by

$$\hat{F}_n(x) := \frac{1}{n} \sum_{i=1}^n \mathbf{1}\{X_i \leq x\}.$$

211 Then, for any  $\varepsilon > 0$ ,

$$\mathbb{P}\left(\sup_{x \in \mathbb{R}} |\hat{F}_n(x) - F^*(x)| > \varepsilon\right) \leq 2e^{-2n\varepsilon^2}.$$

212 Equivalently, for any confidence level  $\delta \in (0, 1)$ , with probability at least  $1 - \delta$ ,

$$\sup_{x \in \mathbb{R}} |\hat{F}_n(x) - F^*(x)| \leq \sqrt{\frac{1}{2n} \log\left(\frac{2}{\delta}\right)}.$$

213 **Lemma A.2** [*Hoeffding (additive) via [7]*]

214 Let  $Z_1, \dots, Z_n \in [0, 1]$  be independent,  $T = \sum_{i=1}^n Z_i$ , and  $\mu = \mathbb{E}[T]$ . For any  $t \in [0, \mu]$ ,

$$\mathbb{P}(T \leq \mu - t) \leq \exp\left(-\frac{2t^2}{\sum_{i=1}^n (1 - 0)^2}\right) = \exp\left(-\frac{2t^2}{n}\right).$$

215 **Lemma A.3** [*Chernoff–Hoeffding for one-parameter exponential family*]

216 Let  $X_1, \dots, X_n$  be i.i.d. with density (or mass) in the one-parameter canonical exponential family

$$p_\theta(x) = \exp\{\theta T(x) - A(\theta)\} h(x), \quad \theta \in \Theta,$$

217 where  $T(x)$  is the sufficient statistic,  $A(\theta)$  is the log-partition function (convex, differentiable on  $\Theta$ ),  
 218 and the mean map is  $\mu(\theta) := \mathbb{E}_\theta[T(X)] = A'(\theta)$ . Assume  $\Theta$  is an open interval and all quantities  
 219 below are finite.

220 Define the empirical mean of the sufficient statistic

$$\bar{T}_n = \frac{1}{n} \sum_{i=1}^n T(X_i).$$

221 For each  $t$  in the range of  $\bar{T}_n$  let  $\theta_t$  be the (unique) canonical parameter satisfying  $\mu(\theta_t) = t$ . Then  
 222 for any  $\varepsilon > 0$ ,

$$\mathbb{P}(D(p_{\theta_{\bar{T}_n}} \| p_\theta) > \varepsilon) \leq 2e^{-n\varepsilon}, \quad \text{or equivalently, } \mathbb{P}(D(p_{\hat{\theta}_n} \| p_\theta) > \varepsilon) \leq 2e^{-n\varepsilon}.$$

223 *Proof:*

224 Define the shifted log-MGF under  $p_\theta$ ,

$$\psi_\theta(\lambda) := \log \mathbb{E}_\theta[e^{\lambda T(X)}] = A(\theta + \lambda) - A(\theta),$$

225 where the displayed equality follows from the exponential-family form (for  $\lambda$  in the domain where  
 226 the expectation is finite). For an attainable mean  $m$  denote  $\theta_m$  as the unique solution of  $\mu(\theta_m) = m$ .

227 By adopting the one-sided Chernoff bound, for any real  $\lambda$  such that expectations exist and any  $m \in \mathbb{R}$ ,

$$\mathbb{P}_\theta(\bar{T}_n \geq m) = \mathbb{P}(e^{\lambda n \bar{T}_n} \geq e^{\lambda n m}) \leq e^{-\lambda n m} \mathbb{E}_\theta[e^{\lambda n \bar{T}_n}] = \exp(-n(\lambda m - \psi_\theta(\lambda))).$$

228 Optimizing over  $\lambda$  gives the Chernoff bound

$$\mathbb{P}_\theta(\bar{T}_n \geq m) \leq \exp(-n\psi_\theta^*(m)), \quad \psi_\theta^*(m) := \sup_{\lambda \in \mathbb{R}} \{\lambda m - \psi_\theta(\lambda)\},$$

229 where  $\psi_\theta^*(m)$  is the Fenchel-Legendre transform of log-MGF. A symmetric argument with  $\lambda < 0$   
 230 yields the lower-tail bound

$$\mathbb{P}_\theta(\bar{T}_n \leq m) \leq \exp(-n\psi_\theta^*(m)).$$

231 We next link the Fenchel-Legendre transform to KL-Divergence using exponential tilting. First,  
 232 adopting change of variables  $\eta = \theta + \lambda$ . Then

$$\psi_\theta^*(m) = \sup_{\eta} \{\langle \eta - \theta, m \rangle - (A(\eta) - A(\theta))\} = A(\theta) + A^*(m) - \langle \theta, m \rangle,$$

233 where  $A^*(m) = \sup_{\eta} \{\langle \eta, m \rangle - A(\eta)\}$  is the convex conjugate of  $A$ . When  $m$  is attainable, the  
 234 supremum is achieved at  $\eta = \theta_m$ , and therefore

$$\psi_\theta^*(m) = \langle \theta_m - \theta, m \rangle - (A(\theta_m) - A(\theta)).$$

235 But for exponential-family densities one has the following direct algebraic identity for the KL:

$$\begin{aligned} D(p_{\theta_1} \| p_{\theta_2}) &= \mathbb{E}_{\theta_1} \left[ \log \frac{p_{\theta_1}(X)}{p_{\theta_2}(X)} \right] \\ &= \mathbb{E}_{\theta_1} [(\theta_1 - \theta_2)T(X) - (A(\theta_1) - A(\theta_2))] \\ &= (\theta_1 - \theta_2) \mathbb{E}_{\theta_1}[T(X)] - (A(\theta_1) - A(\theta_2)). \end{aligned}$$

236 Taking  $\theta_1 = \theta_m$  and  $\theta_2 = \theta$  (so  $\mathbb{E}_{\theta_1}[T] = m$ ) yields

$$\psi_\theta^*(m) = D(p_{\theta_m} \| p_\theta).$$

237 Combining this with the one-sided Chernoff-bound above yields the one-sided KL-form Chernoff  
 238 bounds

$$\mathbb{P}_\theta(\bar{T}_n \geq m) \leq e^{-nD(p_{\theta_m} \| p_\theta)}, \quad \mathbb{P}_\theta(\bar{T}_n \leq m) \leq e^{-nD(p_{\theta_m} \| p_\theta)}.$$

239 Fix  $\varepsilon > 0$ . Because  $A'' > 0$  the function  $m \mapsto D(p_{\theta_m} \| p_\theta)$  is continuous, strictly convex and has a  
 240 unique minimum 0 at  $m = A'(\theta)$ . Thus the sublevel set  $\{m : D(p_{\theta_m} \| p_\theta) < \varepsilon\}$  is an open interval  
 241  $(m_-, m_+)$ ; equivalently

$$\{m : D(p_{\theta_m} \| p_\theta) \geq \varepsilon\} = (-\infty, m_-] \cup [m_+, \infty).$$

242 Hence

$$\{D(p_{\theta_{\bar{T}_n}} \| p_\theta) \geq \varepsilon\} \subseteq \{\bar{T}_n \leq m_-\} \cup \{\bar{T}_n \geq m_+\}.$$

243 Applying the one-sided KL bounds at  $m_\pm$  (each equals  $\varepsilon$ ) and using the union bound gives

$$\mathbb{P}(D(p_{\theta_{\bar{T}_n}} \| p_\theta) \geq \varepsilon) \leq e^{-n\varepsilon} + e^{-n\varepsilon} = 2e^{-n\varepsilon},$$

244 which proves the lemma.

245 **Lemma A.4 (Chernoff-Hoeffding Inequality)**

246 Let  $X_1, \dots, X_n \sim \text{Ber}(\tilde{p})$  be i.i.d. Bernoulli random variables with unknown mean  $\tilde{p}$ , and define the  
 247 empirical mean as

$$\bar{X}_n = \frac{1}{n} \sum_{i=1}^n X_i.$$

248 Then for any  $\varepsilon > 0$ ,

$$\mathbb{P}(D(\bar{X}_n \| \tilde{p}) > \varepsilon) \leq 2e^{-n\varepsilon},$$

249 where  $D(p \| q)$  is the Kullback–Leibler divergence between Bernoulli distributions with parameters  
 250  $p$  and  $q$ .

251 *Proof:* Via Lemma A.3

252 **Lemma A.5 (Multinomial Chernoff-Hoeffding Bound via [11])** For all  $d \leq (\frac{nC_0}{4})^{\frac{1}{3}}$  and  $P \in$   
 253  $\mathcal{M}_k$ , the following holds with the universal constants  $C_0 = \frac{e^3}{2\pi} \approx 3.1967$ , for any  $\epsilon > 0$ ,

$$\Pr(D(\widehat{P}_{n,d} \| P) \geq \epsilon) \leq 2(d-1)e^{-\frac{n\epsilon}{d-1}}.$$

254 **Lemma A.6 (Order-statistic thresholding)** Let  $x_1, \dots, x_m \in \mathbb{R}$  and let  $x_{(1)} \leq \dots \leq x_{(m)}$  be  
 255 their order statistics. Fix a threshold  $\tau \in \mathbb{R}$  and an integer  $N \in \{1, \dots, m\}$ . If at least  $N$  of the  
 256 sample values are at least  $\tau$ , i.e.  $|\{j : x_j \geq \tau\}| \geq N$ , then

$$x_{(m-N+1)} \geq \tau.$$

257 (Equivalently, if at least  $N$  of the  $x_j$  are strictly larger than  $\tau$ , the same conclusion holds.)

258 *Proof:*

259 Suppose, for contradiction, that  $x_{(m-N+1)} < \tau$ . Then all of the first  $m - N + 1$  order statistics  
 260 are strictly less than  $\tau$ , so there are at most  $m - (m - N + 1) = N - 1$  indices  $j$  with  $x_j \geq \tau$ ,  
 261 contradicting  $|\{j : x_j \geq \tau\}| \geq N$ . Hence  $x_{(m-N+1)} \geq \tau$ .

## 262 B Simulation System Examples

263 **Manufacturing: Factory Production (discrete-event simulation; cycle time).**

- 264 • Outcome space:  $\mathcal{X} = \mathbb{R}_+$  (cycle time or throughput).
- 265 • Scenarios:  $\psi =$  product mix + scheduling policy + shift plan.
- 266 • Profiles:  $\mathcal{Z} =$  machine/operator states, shift team, lot sizes;  $\mathcal{P} =$  plant variability.
- 267 • Laws:  $Q^{\text{gt}}(\cdot | z, \psi) =$  empirical cycle-time distribution on the floor;  $Q^{\text{sim}}(\cdot | a(z), \psi, r) =$   
 268 DES output under mirrored inputs.
- 269 • Parameters:  $\Theta = \mathbb{R}$  (mean cycle time) or  $\mathbb{R}^2$  (mean, variance).
- 270 • Discrepancy:  $L =$  difference of means, Gaussian KL.
- 271 • Sampling:  $n_j$  production runs logged;  $k$  simulated replications per scenario.

272 **Environment: Urban decarbonization (technology choice; multinomial).**

- 273 • Outcome space:  $\mathcal{X} = \{1, \dots, K\}$  with mean  $p(\psi) \in \Delta^{K-1}$  (for example,  
 274 {gas furnace, heat pump, variable refrigerant flow, other}).
- 275 • Scenarios:  $\psi$  consists of city, season, rebate level, carbon price path, and policy bundle.
- 276 • Profiles:  $\mathcal{Z}$  contains household and building attributes such as income, occupants, roof area,  
 277 and baseline electricity use, or exogenous drivers including weather and demand shocks.
- 278 • Laws:  $Q^{\text{gt}}(\cdot | z, \psi)$  denotes the empirical technology-choice distribution, and  $Q^{\text{sim}}(\cdot |$   
 279  $a(z), \psi, r)$  denotes the simulator output under mirrored inputs.
- 280 • Parameters:  $\Theta = \Delta^{K-1}$  for category probabilities, or a low-dimensional reparameterization  
 281 such as multinomial logistic parameters.
- 282 • Discrepancy:  $L$  on the simplex, for example the total-variation distance  $\frac{1}{2}\|p - q\|_1$ , the  
 283 multiclass Kullback–Leibler divergence  $\sum_{c=1}^K p_c \log(p_c/q_c)$ .
- 284 • Sampling:  $n_j$  human records per scenario and  $k$  synthetic replications per scenario.

## 285 C Proof to Theorem 3.1

286 We first prove the fixed level of confidence  $\bar{\alpha}$  case.

287 As a setup, we work conditionally on  $\mathcal{G}_j := \sigma(\psi_j, \hat{q}_j, n_j)$ ,  $\mathcal{G} := \sigma(\{\mathcal{G}_j\}_{j=1}^m)$ . For brevity, we abuse  
 288 notation and write  $p(\psi_j)$ ,  $q(\psi_j)$  as  $p_j$ ,  $q_j$ , and similarly  $\hat{p}$ ,  $\hat{q}$ . In addition, for any quantities  $\{\Delta_j\}_{j=1}^m$ ,



289 we denote the sorted version as  $\{\Delta_{(i)}\}_{i=1}^m$ , ie.  $\Delta_{(1)} \leq \dots \leq \Delta_{(m)}$ . For any sequence  $\{\Delta_j\}_{j=1}^m$ , let  
 290  $\Delta_{(1)} \leq \dots \leq \Delta_{(m)}$  denote its order statistics. Throughout the proof,  $\alpha \in (0, 1)$  denotes a generic  
 291 quantile index (a function argument) and is distinct from the target coverage level  $\bar{\alpha}$ .

292 We seek the quantile function of  $\Delta_j = L(p_j, q_j)$ , but only observe the estimators  $(\hat{p}_j, \hat{q}_j)$ . To  
 293 preserve an i.i.d. structure, we instead work with the proxy  $\bar{\Delta}_j := L(p_j, \hat{q}_j)$ , for which the sequence  
 294  $\{\bar{\Delta}_j\}_{j=1}^m$  is i.i.d., since we fix the simulator budget  $k$  and each scenarios  $\{\psi_j\}$  are i.i.d. as assumed  
 295 in Section 2.

296 By defining  $\bar{V}_m(\alpha)$  as an empirical  $\alpha$  quantile of  $\{\bar{\Delta}_j\}_{j=1}^m$ , formally  $\bar{V}_m(\alpha) = \inf\{t : \bar{F}_m(t) \geq$   
 297  $\alpha\} = \bar{\Delta}_{(\lceil m\alpha \rceil)}$  for the ordered  $\bar{\Delta}_{(i)}$ , where  $\bar{F}_m(t) = \frac{1}{m} \sum_{j=1}^m \mathbb{I}(\bar{\Delta}_j \leq t)$ . If we have access to  
 298  $\bar{V}_m(\alpha)$ , then we can claim, by Lemma A.1, that with probability  $1 - \delta$ :

$$\mathbb{P}_{\psi \sim \Psi}(L(p(\psi), \hat{q}(\psi)) \leq \bar{V}_m(1 - \frac{\bar{\alpha}}{2}) | \mathcal{D}) \geq 1 - \frac{\bar{\alpha}}{2} - \sqrt{\frac{\log(2/\delta)}{2m}} \quad (1)$$

299 and this would deliver our desired envelope bound.

300 However, we do not have access to  $p_j$ , so we need to estimate it with  $\hat{p}_j$ . If we are in the case of  
 301  $n_j = n$ , then this can be solved by creating an uncertainty set across all  $j$ . Specifically, we take  
 302 sup  $L$  out of an uncertainty set over  $\hat{p}_j$  that ensures with high probability  $p_j$  lies inside, and because  
 303  $n_j$ s are identical this quantity is still i.i.d. , hence the above procedure is still valid. This leads to  
 304 another problem, which is that we do not have the same sample size  $n_j$  for each  $\psi_j$ , so  $L(\hat{p}_j, \hat{q}_j)$  will  
 305 not be i.i.d. , so we need to try to control for this heterogeneity.

We instead construct a randomized pseudo-divergences with respect to  $\bar{\Delta}_j$ . Specifically, we allow a  
 randomized level of coverage  $\gamma_j \sim \text{Unif}(0, 1)$ ,  $\forall j \in [m]$ , and define the two divergence terms as

$$\begin{cases} \bar{\Delta}_j = L(p_j, \hat{q}_j) & , \text{i.i.d., yet unobservable} \\ \hat{\Delta}_j := \sup_{u \in \mathcal{C}_j(\hat{p}_j, \gamma_j)} L(u, \hat{q}_j) & , \text{Not i.i.d., yet observable,} \end{cases}$$

306 where  $\mathcal{C}_j(\hat{p}_j, \gamma_j) \subset \Theta$  are data-driven confidence sets satisfying  $\mathbb{P}(p_j \in \mathcal{C}_j(\hat{p}_j, \gamma_j) | \psi_j, n_j) \geq \gamma_j$ .

307 By Assumption 2 and the compactness of the confidence set  $\mathcal{C}_j(\hat{p}_j, \gamma_j) \subset \Theta$ , Berge's maximum  
 308 theorem guarantees that the supremum in the definition of  $\hat{\Delta}_j$  is attained, hence  $\hat{\Delta}_j$  is well defined.  
 309 Therefore, by the coverage property of  $\mathcal{C}_j$ , we have

$$\mathbb{P}(\hat{\Delta}_j \geq \bar{\Delta}_j | \mathcal{G}_j \cup \sigma(\gamma_j)) \geq \gamma_j,$$

310 and if we marginalize over  $\gamma_j$ , by  $\gamma_j \perp\!\!\!\perp \mathcal{G}_j$  we get  $\forall j$

$$\begin{aligned} \mathbb{P}(\hat{\Delta}_j \geq \bar{\Delta}_j | \mathcal{G}_j) &= \mathbb{E}[\mathbb{P}(\hat{\Delta}_j \geq \bar{\Delta}_j | \mathcal{G}_j \cup \sigma(\gamma_j) | \mathcal{G}_j)] \\ &\geq \mathbb{E}[\gamma_j | \mathcal{G}_j] = \frac{1}{2}. \end{aligned} \quad (2)$$

311 Furthermore, by the tower property and independence of  $\gamma_j$  from  $\mathcal{G}_j$ ,

$$\mathbb{P}(\hat{\Delta}_j \geq \bar{\Delta}_j) = \mathbb{E}[\mathbb{P}(\hat{\Delta}_j \geq \bar{\Delta}_j | \mathcal{G}_j)] \geq \frac{1}{2},$$

312 and, conditionally on  $\mathcal{G}$ , the indicators  $Y_j = \mathbf{1}\{\hat{\Delta}_j \geq \bar{\Delta}_j\}$  are independent across  $j$ .

313 We will now use  $\{\hat{\Delta}_j\}_{j=1}^m$  to create an upper bound of  $\bar{V}_m(1 - \alpha)$ , which along side (1) will give us  
 314 our desired envelope. Intuitively, we want to find a larger quantile of  $\hat{\Delta}_j$  and with (2), we can claim  
 315 an upper bound of  $\bar{V}_m(1 - \alpha)$  with high probability.

316 First, we define an imaginary set  $S_\alpha = \{j \in [m] : \bar{\Delta}_j \geq \bar{V}_m(1 - \alpha)\}$ , and denote  $|S_\alpha| = s$ . By  
 317 definition of empirical  $1 - \alpha$  quantile,  $\inf k = \lceil m(1 - \alpha) \rceil$ , and hence

$$s = m - k + 1 = m - \lceil m(1 - \alpha) \rceil + 1 \geq \lfloor m\alpha \rfloor + 1.$$

318 We next define  $Y_j = \mathbb{I}(\hat{\Delta}_j \geq \bar{\Delta}_j)$ . By (2):  $\mathbb{P}(Y_j = 1 | \mathcal{G}) \geq \frac{1}{2}$ . We now define another imaginary set  
 319  $T_\alpha = \{j \in S_\alpha : \hat{\Delta}_j \geq \bar{\Delta}_j\} = \{j \in S_\alpha : Y_j = 1\} = \{j : \hat{\Delta}_j \geq \bar{\Delta}_j \geq \bar{V}_m(1 - \alpha)\}$ , with which we  
 320 use to choose our upper bound. First we calculate  $\mathbb{E}[T_\alpha]$ :

$$\mathbb{E}[T_\alpha | \mathcal{G}] = \mathbb{E}\left[\sum_{j \in S_\alpha} Y_j | \mathcal{G}\right] = \sum_{j \in S_\alpha} \mathbb{P}(Y_j | \mathcal{G}) \geq \frac{1}{2}s.$$

321 Lemma A.2 implies that for any  $\delta \in [0, \frac{1}{2}s]$ , we have:

$$\mathbb{P}(|T_\alpha| \leq \frac{1}{2}s - t | \mathcal{G}) \leq \mathbb{P}(|T_\alpha| \leq \mathbb{E}[T_\alpha] - t | \mathcal{G}) \leq \exp(-\frac{2t^2}{s}),$$

322 where we applied  $\mathbb{E}[T_\alpha | \mathcal{G}] \geq \frac{1}{2}s$  in the first inequality. By setting  $t = c\sqrt{s}$ :

$$\mathbb{P}(|T_\alpha| \leq \frac{1}{2}s - t | \mathcal{G}) \leq \exp(-2c^2) \quad (3)$$

323 With this bound, we can link the actual set of indices we have interest, ie.  $U_\alpha = \{j : \hat{\Delta}_j \geq$   
 324  $\bar{V}_m(1 - \alpha)\}$  to  $T_\alpha$ . By construction,  $T_\alpha \subseteq U_\alpha$ , hence by (3), with probability greather than  
 325  $1 - \exp(-2c^2)$ :

$$|U_\alpha| \geq |T_\alpha| \geq \frac{1}{2}s - c\sqrt{s},$$

326 which implies at least  $\frac{1}{2}s - c\sqrt{s}$  of the  $\hat{\Delta}_j$ 's are larger than  $\bar{V}_m(1 - \alpha)$  with high probability.

327 We now analyze: for a fixed  $\alpha$ , what coverage guarantee can we get for the inner probability via  
 328 order statistics. Set  $N := \lfloor \frac{1}{2}s - c\sqrt{s} \rfloor$ . If at least  $N$  sample values exceed  $\bar{V}_m(1 - \alpha)$ , then by  
 329 order-statistics calculus (Lemma A.6)

$$\hat{V}_m(1 - \alpha) = \hat{\Delta}_{(m - \lfloor m\alpha \rfloor)} \geq \bar{V}_m(1 - \alpha_{\text{eff}}),$$

330 whenever  $\alpha_{\text{eff}}$  is chosen so that  $N \geq \lfloor m\alpha \rfloor + 1$  holds when  $s \geq \lfloor m\alpha_{\text{eff}} \rfloor + 1$ .

331 A sufficient condition is

$$\frac{1}{2}m\alpha_{\text{eff}} - c\sqrt{m\alpha_{\text{eff}}} - 1 \geq m\alpha.$$

332 Define  $\alpha_{\text{eff}}(\alpha, c, m) := \inf\{x \in (0, 1) : \frac{1}{2}x - c\sqrt{\frac{x}{m}} - \frac{1}{m} \geq \alpha\}$ . Writing  $y = \sqrt{x}$ , this is equivalent  
 333 to  $y^2 - \frac{2c}{\sqrt{m}}y - (\frac{2}{m} + 2\alpha) \geq 0$ , so the minimal admissible  $y$  is

$$y^* = \frac{2c/\sqrt{m} + \sqrt{4c^2/m + 8\alpha + 8/m}}{2}, \quad \alpha_{\text{eff}}(\alpha, c, m) = (y^*)^2.$$

334 Thus we obtain the comparison event

$$\mathcal{E}_\alpha := \left\{ \hat{V}_m(1 - \alpha) \geq \bar{V}_m(1 - \alpha_{\text{eff}}(\alpha, c, m)) \right\}, \quad \mathbb{P}(\mathcal{E}_\alpha) \geq 1 - e^{-2c^2}. \quad (4)$$

335 Apply (1) at level  $1 - \alpha_{\text{eff}}(\alpha, c, m)$ :

$$\mathbb{P}_{\psi \sim \Psi}(L(p(\psi), \hat{q}(\psi)) \leq \bar{V}_m(1 - \alpha_{\text{eff}}) | \mathcal{D}) \geq 1 - \alpha_{\text{eff}}(\alpha, c, m) - \varepsilon_m(\delta).$$

336 On  $\mathcal{E}_\alpha$  in (4),  $\bar{V}_m(1 - \alpha_{\text{eff}}) \leq \hat{V}_m(1 - \alpha)$ . Hence,

$$\mathbb{P}_{\psi \sim \Psi}(L(p(\psi), \hat{q}(\psi)) \leq \hat{V}_m(1 - \alpha) | \mathcal{D}) \geq 1 - \alpha_{\text{eff}}(\alpha, c, m) - \varepsilon_m(\delta),$$

337 with outer probability at least  $1 - \delta - e^{-2c^2}$ .

338 The exact algebraic form is

$$\alpha_{\text{eff}}(\alpha, c, m) = \frac{\left(\frac{2c}{\sqrt{m}} + \sqrt{\frac{4c^2}{m} + 8\alpha + \frac{8}{m}}\right)^2}{4} = 2\alpha + \frac{c}{\sqrt{m}}\sqrt{8\alpha + \frac{4c^2+8}{m}} + \frac{2c^2+2}{m},$$

339 and, as  $m \rightarrow \infty$ ,  $\alpha_{\text{eff}}(\alpha, c, m) = 2\alpha + c\sqrt{8\alpha/m} + O(m^{-1})$ .

340 Finally,  $\mathbb{P}_{\psi \sim \Psi}(\cdot | \mathcal{D})$  is over a fresh test scenario given the realized calibration data  $\mathcal{D}$ . High-  
 341 probability qualifiers are taken over  $(\mathcal{D}, \{\gamma_j\})$ . We first condition on  $\mathcal{G}$  (leaving  $\{\hat{p}_j\}, \{\gamma_j\}$  random),  
 342 derive conditional bounds, and then remove the conditioning via the tower property; both key events  
 343 (1) and (4) are measurable in  $(\mathcal{D}, \{\gamma_j\})$ .

344 We have shown that for any target level  $\alpha$  and choice of  $c > 0$ , the preceding argument yields a  
 345 high-probability concentration bound based on  $\{\hat{\Delta}_j\}_{j=1}^m$ . We now extend the guarantee to hold  
 346 *uniformly* over all  $\alpha$ . Fix  $c > 0$  and  $\delta \in (0, 1)$ . For the grid  $\alpha_r := r/m$  ( $r = 1, \dots, m$ ), let

$$\mathcal{E}_{\text{DKW}} := \left\{ \sup_x |\hat{F}_m(x) - F^*(x)| \leq \varepsilon_m(\delta) \right\}, \quad \mathcal{E}_r := \left\{ (3.1) \text{ holds with } \alpha = \alpha_r \right\}.$$

347 By DKW,  $\Pr(\mathcal{E}_{\text{DKW}}) \geq 1 - \delta$ , and by the fixed-level argument,  $\Pr(\mathcal{E}_r) \geq 1 - e^{-2c^2}$  for each  $r$ .  
 348 Hence, by a union bound,

$$\Pr\left(\mathcal{E}_{\text{DKW}} \cap \bigcap_{r=1}^m \mathcal{E}_r\right) \geq 1 - \delta - me^{-2c^2}.$$

349 Work on the event  $\mathcal{E}_{\text{DKW}} \cap \bigcap_{r=1}^m \mathcal{E}_r$ . For any  $\alpha \in (0, 1)$  let  $r = \lceil m\alpha \rceil$  and denote  $\alpha_+ := \alpha_r =$   
 350  $r/m \in [\alpha, \alpha + 1/m]$ . Since the empirical quantile is piecewise constant on the  $m$ -grid,

$$\hat{V}_m(1 - \alpha) = \hat{V}_m(1 - \alpha_+).$$

351 Applying (3.1) at level  $\alpha_+$  yields

$$\mathbb{P}_{\psi \sim \Psi}\left(\Delta(\psi) \leq \hat{V}_m(1 - \alpha) \mid \mathcal{D}\right) \geq 1 - 2\alpha_+ - \frac{c}{\sqrt{m}} \sqrt{8\alpha_+ + \frac{4c^2 + 8}{m}} - \frac{2c^2 + 2}{m} - \varepsilon_m(\delta).$$

352 Since  $\alpha_+ \in [\alpha, \alpha + 1/m]$  and the right-hand side is nonincreasing in  $\alpha$ , the same bound holds with  
 353  $\alpha$  replaced by  $\alpha_+$ , and (optionally) one may absorb the rounding slack  $\alpha_+ - \alpha \leq 1/m$  into the  
 354  $O(m^{-1})$  term by a crude inequality

$$2\alpha_+ \leq 2\alpha + \frac{2}{m}, \quad \sqrt{8\alpha_+ + \frac{4c^2 + 8}{m}} \leq \sqrt{8\alpha + \frac{4c^2 + 16}{m}}.$$

355 Therefore, with probability at least  $1 - \delta - me^{-2c^2}$  over  $\mathcal{D}$ , the guarantee (3.1) (at  $\alpha$  replaced by  
 356  $\alpha_+$ ) holds *uniformly* for all  $\alpha \in (0, 1)$ . The form in the main theorem is a mere simplification with  
 357 respect to  $c$  and  $\delta$ .

## 358 D Additional Applications: EEDI Dataset

359 We apply the methodology from Section 3 to real data. Our primary dataset is EEDI [6], built on  
 360 the NeurIPS 2020 Education Challenge [19], which consists of student responses to mathematics  
 361 multiple-choice questions collected on the Eedi online education platform. The full corpus includes  
 362 573 distinct questions and 443,433 responses from 2,287 students, and each question has four options  
 363 A–D that we binarize as “correct/incorrect” based on the students or simulators choice, consistent  
 364 with Lemma A.4. We adopt the preprocessed version curated by [8], which retains questions with  
 365 at least 100 student responses and excludes items with graphs or diagrams, yielding 412 questions.  
 366 EEDI also provides individual-level covariates such as gender, age, and socioeconomic status, which  
 367 the authors of [8] use to construct synthetic profiles. Under the same problem formulation, they  
 368 compute  $\{\hat{p}_j, \hat{q}_j\}_{j=1}^{412}$  for seven LLMs: GPT-3.5-TURBO (gpt-3.5-turbo), GPT-4o (gpt-4o), and  
 369 GPT-4o-MINI (gpt-4o-mini); CLAUDE 3.5 HAIKU (claude-3-5-haiku-20241022); LLAMA  
 370 3.3 70B (Llama-3.3-70B-Instruct-Turbo); MISTRAL 7B (Mistral-7B-Instruct-v0.3);  
 371 DEEPSEEK-V3 (DeepSeek-V3), and constructed a benchmark random simulator that selects uni-  
 372 formly among the available answer choices. A more detailed exploration into the EEDI dataset and  
 373 the simulation procedure can be found in [8].

374 We apply our methodology to produce a fidelity profile for each candidate LLM  $\ell$ . We use absolute  
 375 error as the loss,  $L(p, q) = |p - q|$ . We set  $\gamma = 0.5$  uniformly and the DKW failure probability to  
 376  $\delta = 0.1$ , which determines the curve’s effective width at  $\alpha \rightarrow 1$  in Figure 2. In addition, we set the  
 377 simulation budget  $k = 50$ .

378 Figure 2 compares models by how tightly their synthetic outcomes track the human distribution across  
 379 items. We plot  $\hat{V}_\ell(\alpha)$  against  $\alpha$ , where lower-flatter curves indicate uniformly small discrepancies,  
 380 while elbows reveal rare but severe misses. DEEPSEEK-V3 lies lowest across most quantiles,  
 381 indicating the most reliable alignment, with the random benchmark and GPT-4o close behind.  
 382 Notably, several models do not outperform the random baseline, suggesting they may be ill-suited for  
 383 agent-based simulation under this discrepancy function.

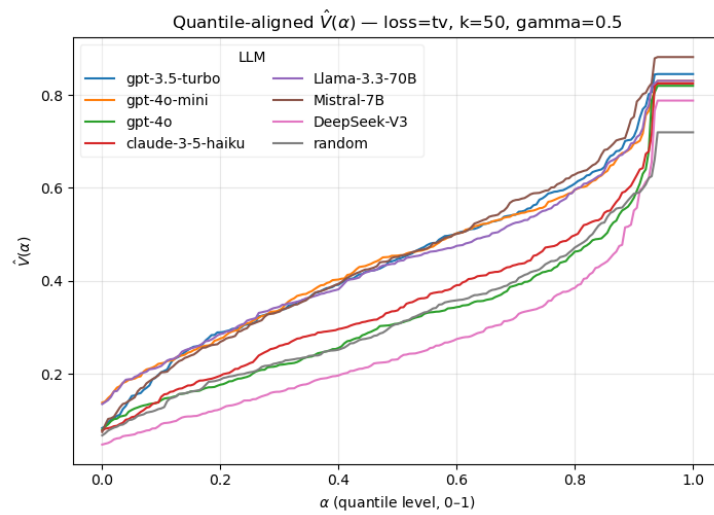


Figure 2: Quantile fidelity profiles  $\hat{V}(\alpha)$  across LLMs (Discrepancy: Absolute loss,  $k = 50$ ,  $\beta = 0.5$ ,  $\delta = 0.1$ ).